The Cryosphere Discuss., 4, 2415–2432, 2010
www.the-cryosphere-discuss.net/4/2415/2010/
doi:10.5194/tcd-4-2415-2010

The Cryosphere Discussions

Photogrammetric determination of spatio-temporal velocity fields at Glaciar San Rafael in the Northern Patagonian Icefield

H.-G. Maas[1], G. Casassa[2], D. Schneider[1], E. Schwalbe[1], and A. Wendt[2]

[1]Institute of Photogrammetry and Remote Sensing, Dresden University of Technology, Dresden, Germany
[2]Centro de Estudios Científicos, Valdivia, Chile

Received: 24 August 2010 – Accepted: 4 October 2010 – Published: 12 November 2010

Correspondence to: H.-G. Maas (hans-gerd.maas@tu-dresden.de)

Published by Copernicus Publications on behalf of the European Geosciences Union.

Abstract

Glaciar San Rafael in the Northern Patagonian Icefield, with a length of 46 km and an ice area of 722 km^2, is the lowest latitude tidewater outlet glacier in the world and one of the fastest and most productive glaciers in southern South America in terms of iceberg flux. In a joint project of the TU Dresden and CECS, spatio-temporal velocity fields in the region of the glacier front were determined in a campaign in austral spring of 2009. Monoscopic terrestrial image sequences were recorded with an intervallometer mode high resolution digital camera over several days. In these image sequences, a large number of glacier surface points were tracked by subpixel accuracy feature tracking techniques. Scaling and georeferencing of the trajectories obtained from image space tracking was performed via a multi-station GPS-supported photogrammetric network.

The technique allows for tracking hundreds of glacier surface points at a measurement accuracy in the order of one decimeter and an almost arbitrarily high temporary resolution. The results show velocities of up to 16 m per day. No significant tidal signals could be observed. Our velocities are in agreement with earlier measurements from theodolite and satellite interferometry performed in 1986–1994, suggesting that the current thinning of 3.5 m/y at the front is not due to dynamic thinning but rather by enhanced melting.

1 Introduction

Glaciar San Rafael at 46°42′ S/73°50′ W is one of the major outlet glaciers of the Northern Patagonian Ice Field in southern Chile. It is the lowest latitude tidewater outlet glacier in the world. The glacier calves into the Laguna San Rafael at sea level (Figs. 1 and 2), which is connected to the Pacific Ocean fjords via the 8 km long Río Témpanos. Both the glacier and the laguna belong to the 17 420 km^2 Laguna San Rafael National Park, a UNESCO biosphere reserve 120 km south of Puerto Chacabuco with elevations up to 4058 m. The area is very wet with a mean annual precipitation of 4440 mm

TCD
4, 2415–2432, 2010

during the years 1981–1985 at the meteorological station of Laguna San Rafael (Lliboutry, 1999). At higher elevations, precipitation increases to up to 7500 mm per year (Escobar et al., 1992).

The glacier has an ice area of 722 km^2 (Rivera et al., 2007) and a length of 46 km (Aniya, 1988). Thanks to historical descriptions of early explorers, the fluctuations of Glaciar San Rafael are known since 1675, at which time the glacier's front was located close to the lake's eastern shore, similar to its present position. From 1675 until the late 18th century, the glacier did not show any relevant advance. During the second half of the 19th century, at the peak of Little Ice Age, the glacier had advanced 8 km into Laguna San Rafael, covering a major portion of lake (Araneda et al., 2007). Since the late 19th century, the glacier front has retreated over a total distance of 14 km, with two periods of smaller advances: 1935–1959 (Heusser, 1960) and 1990–1999 (Warren et al., 1995; Aniya et al., 1998). A retreat of up to 400 m per year during the 1980s year has been reported (Warren, 1993). Within the period 1880–2001 the glacier lost 72 km^2 (Warren, 1993; Rivera et al., 2007). In the past decade, the glacier calving front has been retreating (Rivera et al., 2007; Masiokas et al., 2009) at a steady pace of about 100 linear meters per year, which can also be seen from local markers dating back to 1978. The main driver for the retreat tendency of San Rafael Glacier can be attributed to regional warming (e.g. Rasmussen et al., 2007), while the glacier advances during the 20th century have been explained due to periods of precipitation increase (Warren et al., 1993).

Glacier velocities are fundamental data for understanding the glacier behavior. Several authors have published results of glacier movement velocity measurements. Naruse (1987), Kondo and Yamada (1988) and Warren et al. (1995) performed theodolite triangulation measurements over periods of a few days and determined mean glacier surface velocities of 17 m per day at the calving front, dropping to 13 m per day 500 m behind the front (12 m/d 1.2 km from the front according to Warren, 1995; 11 m/d 1.2 km from the front according to Rignot et al., 1996). Rignot et al. (1996) present one-dimensional interferometric velocities from NASA's Spaceborne Imaging

TCD
4, 2415–2432, 2010

SAR data obtained at an interval of 16.4 days during the 1994 Space Shuttle mission. While the precision of these measurements is very high (5 mm per day), interferometric SAR data processing failed in the fast and rugged snowfree region near the calving front due to loss of phase coherence. Therefore the velocity field measurements were complemented by (less accurate) feature-tracking results near the calving front. They determined velocities of 2.6 m per day near the equilibrium-line altitude, increasing to 17.5 m per day at the calving front.

Warren et al. (1995) derived an average thickness of the glacier tongue at the terminus of 200 m from bathymetry data in the lagoon and ice cliff heights. Thomas (2007) predicts a tide-induced variation of the ice-front velocity of 2 cm per hour.

The main goal of the research work presented here was the determination spatio-temporal velocity fields near the calving front with high spatial and temporal resolution. For this purpose, a camera was installed at the northern hillside of the glacier to take image sequences similarly to the implementation shown by Maas et al. (2008). The camera system will be briefly shown in Sect. 2. Glacier surface features were tracked by subpixel accuracy least-squares-matching (Sect. 3). The image space trajectories were scaled to the glacier surface via the results of a GPS-supported multi-station photogrammetric network (Sect. 4). Results are shown in Sect. 5.

2 Camera setup

Monoscopic terrestrial image sequences were recorded with an intervallometer mode (also referred to as time-lapse mode) high resolution digital camera over several days. The camera was a Nikon D300 with a 4288×2848 pixel CMOS sensor, equipped with a 28 mm lens which yields an opening angle of 46°. The camera was programmed to take images in 15 min intervals. The camera was installed on a tribrach which was fixedly screwed to the rock. In the ideal case, the camera should be oriented perpendicularly to the glacier motion direction. Due to restrictions posed by the local topography, this perpendicularity could not perfectly be achieved when aspiring maximum glacier

TCD
4, 2415–2432, 2010

coverage of the camera field of view. This deviation from perpendicularity (26.5°) has to be regarded when deriving actual glacier motion velocities from image space measurements. Some fiducials in the image foreground were used to allow for a compensation of possible camera movements, which cannot be completely avoided due to the plastic body of the camera. The image sequences were recorded in March/April 2009.

Basically, determining 3-D glacier surface feature trajectories would require a stereoscopic camera setup. In our implementation, a monoscopic setup was preferred over a stereoscopic setup for several reasons: The main reason for avoiding stereo was the extremely rugged glacier surface (Fig. 3), which made it very difficult to determine homologous points in stereo views, either interactively or automatically by applying image matching techniques. A stereo baseline would have to be in the order of 500 to 1000 m to obtain a good stereo ray intersection warranting a good precision in all three coordinate components of the glacier surface feature trajectories. At this baselength, it was in most cases impossible to detect homologous points in the images. Moreover, local topographic constraints hampered stereo setups with reasonable intersection geometry. Therefore we chose a monoscopic setup and determined 2-D glacier surface feature trajectories in a plane perpendicular to the camera viewing direction, corrected by projection effects caused by the non-perpendicular viewing direction. This 2-D approach is also justified by the fact that there will usually be no significant across track components in the glacier motion field. The monoscopic setup necessitates the determination of a scale factor for each image space trajectory, which is outlined in Sect. 4.

3 Glacier surface feature tracking

Figure 3 shows one image out of an image sequence. In these image sequences, a large number of glacier surface points can be tracked by subpixel accuracy feature tracking techniques. We used least-squares-matching (LSM) to establish correspondences between surface patches in consecutive images. LSM applies 2 to 6 parameters of an affine transformation between two image patches to minimize the sum of

TCD
4, 2415–2432, 2010

the squares of greyvalue differences. It will usually converge to the correct solution in a few iterations. The analysis of the LSM covariance matrix allows deriving an estimate on the translation vector precision. Under good circumstances, LSM may deliver a precision of 1/50 pixel or even better. With the rugged glacier surface and varying illumination conditions, though, the precision will often be significantly worse than this.

To be able to correct the image space trajectories for possible camera movement effects, some fiducials in the image foreground were tracked using the same technique. Camera movements of up to 0.7 pixel were detected and applied to correct the trajectories.

4 Trajectory georeferencing

The monoscopic image space trajectories have to be scaled to the glacier surface in order to determine glacier velocities. The glacier surface shows large height differences and a temporary changing elevation model, and the camera images represent a rather oblique view onto the glacier surface. As a consequence, there are strong variations in the image scale, introduced by both projective and perspective effects. This necessitates the determination of an individual scale factor for each tracked glacier point in order to translate its trajectory from image space to the glacier surface.

This task was accomplished by establishing a GPS-supported multi-station photogrammetric network. A total of 5 images were taken from locations along the northern hillside (Fig. 4). As the glacier surface and the southern hillside were inaccessible, no control points for georeferencing (or at least scaling) the network could be established. Instead, the coordinates of the 5 camera projection centers were determined by GPS. With a non-linear arrangement of the 5 projection centers (Figs. 4 and 5), this basically allows for a full geo-referencing of the photogrammetric network, though at a poor error propagation especially in the vertical coordinate direction. Therefore, additionally some visible points along the waterline of the Laguna San Rafael (representing sea level) were measured in the images of the multi-station photogrammetric network to support the georeferencing.

TCD
4, 2415–2432, 2010

Summing up, the bundle adjustment of the photogrammetric network was based on the following information:

- Image coordinates of glacier surface points (those points which were tracked in the image sequences), used as tie points.
- Further tie points on the southern hillside.
- Water level points at the Laguna San Rafael introduced as height control points.
- GPS measurements of the camera projection centers.
- Camera pre-calibration parameters.

An automatic determination of homologous points in glacier surface images from different views turned out to be impossible as a consequence of the extremely rugged surface pattern. Therefore the tie point coordinates were measured interactively in Photomodeler (Eos Systems Inc.). The further processing in Photomodeler was constrained by the limited datum definition options in the software package. Moreover, the bundle adjustment in Photomodeler turned out to deliver rather instable results. Therefore the measurements were imported to our own bundle adjustment software package (Schneider and Maas, 2007). The standard deviation of unit weight produced by the bundle adjustment was 1.3 pixel, which corresponds to the expectations considering the manual tie point measurements and the interpretation difficulties. Due to the network configuration, the glacier surface point standard deviation depends on the distance of the points from the camera base, increasing approximately with the square of the distance. On average, a standard deviation of 3.3/4.3/0.4 m was obtained for the X/Y/Z coordinates of the glacier surface points in a local coordinate system with the camera viewing direction approximately in the Y-direction. The better value in the Z-direction can be explained by the water level height control points. As the results of the bundle adjustment are only used for scaling the image space trajectories, the obtained accuracy is more than sufficient.

TCD
4, 2415–2432, 2010

Scaling information for each glacier surface point can be derived from its 3-D coordinates and the camera parameters. These scale factors can then be used to translate the glacier surface point trajectories from image space to the glacier surface. Errors from the bundle adjustment will propagate as a linear scale factor into the trajectories. From the results of the bundle adjustment, an average scale error of 0.4% can be estimated.

5 Results

Some glacier surface point velocity vectors obtained from the data processing chain as outlined in the previous sections are shown in Fig. 6. The maximum movement of points close to the glacier front was 16 m per day, dropping to 6–7 m per day some 800 m behind the glacier front.

One camera pixel corresponds to 20 cm on the glacier surface at a distance of 1000 m. The least squares tracking procedure yielded translation parameter standard deviations between 0.004 pixel and 0.08 pixel with an rms of 0.015 pixel. Due to the fact that least squares matching is using signals with stochastic properties on both sides of the observation equation, these results can usually be considered too optimistic. Nevertheless, the pure image tracking contribution to the individual trajectory link is in the centimeter-range. The error accumulates with the square-root of the number of trajectory links (with a typical trajectory length of 51 frames). In addition, as outlined in Sect. 4, the trajectory georeferencing scale error has to be considered. The scale error depends on the distance of the glacier surface point to the camera and the number of rays in the photogrammetric network (2 to 5) and is between 0.3% and 1.6% of the trajectory length. Summing up, a well trackable glacier surface point situated in the middle of the glacier close to the glacier front will have a trajectory length standard deviation in the order of 10–20 cm, corresponding to about 1% of the trajectory length.

Thomas (2007) predicted a tide-induced variation of the ice-front velocity of 2 cm per hour, which is about 3% of the average velocity for Glaciar San Rafael. The tidal

TCD
4, 2415–2432, 2010

amplitude at Glaciar San Rafael is typically ± 0.8 m. In a data capture and processing scheme which was similar to the one shown in this paper, Maas et al. (2008) and Dietrich et al. (2008) were able to show clearly significant tidal effects in the vertical component of glacier surface points of Jacobshavn Isbræ Glacier in West Greenland. The accuracy as estimated above should be high enough to unveil these tide-induced motion effects. Nevertheless, in the results of our Glaciar San Rafael image sequence processing, no significant tide-induced effects, neither in absolute movement velocity nor in the vertical component of the glacier tongue motion, could be detected.

The absence of tidal effects suggests that the frontal portion of Glaciar San Rafael is well grounded. Warren et al. (1995) measured a maximum water depth of 272 m at the central part of the Glaciar San Rafael terminus in 1992 and concluded that there glacier might be in near flotation condition. Glaciar San Rafael is thinning at a maximum rate of 3.5 m per year at the front (Rignot et al., 2003), which would make it more buoyant. However, it is also retreating. The lack of tidal effects on the velocity field at San Rafael could indicate that the glacier front is retreating into shallower waters, thus enhancing its grounded nature. As a by-product, the photogrammetric data processing also allows to determine the glacier front height. At Glaciar San Rafael, heights of up to 55 m could be measured. In order to attain buoyancy here, water depths of about 450 m would be required, which are much larger than the values measured by Warren et al. (1995).

Our velocity values are roughly in agreement with those measured in the period 1986–1994 (Naruse, 1987; Kondo and Yamada, 1988; Warren et al., 1995; Rignot et al., 1996). The stability of the velocity field over time suggests that at least in Glaciar San Rafael no significant acceleration/deceleration has taken place, and that the current thinning of 3.5 m per year should be mainly due to enhanced surface melting and perhaps as well to larger water melting at the front, driven by regional warming (Rasmussen et al., 2007). Contrastingly, for instance at Jacobshavn Isbræ Glacier in Greenland shows the relevance of dynamic thinning (i.e. as a result of accelerated flow).

TCD
4, 2415–2432, 2010

6 Conclusions

Monoscopic terrestrial high resolution image sequence processing is a powerful tool to determine spatio-temporal velocity fields on fast moving glaciers. With subpixel precision image analysis and proper georeferencing by a GPS-supported multi-station photogrammetric network, a high glacier surface point trajectory precision can be obtained. For Glaciar San Rafael in the Northern Patagonian Icefield, velocities up to 16 m per day in the region of the calving front were determined in a measurement campaign in March/April 2009. Our velocities agree with those measured in the period 1986–1994 and suggest that no acceleration has occurred at this tidewater glacier, indicating that the present thinning is mainly due to enhanced surface and also submarine melting at the front. While the temporal resolution and accuracy of the method is high enough to resolve small tide-induced variations in the trajectories, no such effects could be detected at Glaciar San Rafael.

Acknowledgements. The research work presented in this paper is the result of a joint project of the CECS in Valdivia, Chile, and TU Dresden, Germany. It was partly funded by the Chilean Fondo Nacional de Desarrollo Científico y Tecnológico (FONDECYT) and the International Bureau of the German Federal Ministry of Education and Research (BMBF). The permit of Conaf (Corporación Nacional Forestal) Chile and the support of their local rangers are also greatly acknowledged. We especially thank Eliana Chong and Stephanie Joyce, who greatly supported us in a rainy field campaign at Glaciar San Rafael.

The joint research project was initiated by Jens Wendt. Jens Wendt died in a plane crash one week after our measurements at Glaciar San Rafael while returning from a laserscanner survey flight to the Nevados de Chillán. This paper is devoted to his commemoration.

TCD
4, 2415–2432, 2010

References

Aniya, M., Naruse, R., Casassa, G., and Rivera, A.: Variations of Patagonian glaciers, South America, utilizing RADARSAT images. Proceedings of the International Symposium on RADARSAT Application Development and Research Opportunity (ADRO), Montreal, Canada, 13–15 October 1998, 1999.

Araneda, A., Torrejón, F., Aguayo, M., Torres, L., Cruces, F., Cisternas, M., and Urrutia, R.: Historical records of San Rafael glacier advances (North Patagonian Icefield): Another clue to 'Little Ice Age' timing in southern Chile?, The Holocene, 17, 987–998, 2007.

Dietrich, R., Maas, H.-G., Baessler, M., Rülke, A., Richter, A., Schwalbe, E., and Westfeld, P.: Jakobshavn Isbræ, West Greenland: Flow velocities and tidal interaction of the front area from 2004 field observations, J. Geophys. Res., 112(f3), F03S21, 2007.

Escobar, F., Vidal, F., Garin, C., and Naruse, R.: Water balance in the Patagonia Icefield, in: Glaciological researches in Patagonia, edited by: Naruse, R., Aniya, M., Japanese Society of Snow and Ice, Data Center for Glacier Research, 109–119, 1992.

Heusser, C.: Late-Pleistocene environments of the Laguna de San Rafael area, Chile, Geogr. Rev., 50, 555–77, 1960.

Kondo, H. and Yamada, T.: Some remarks on the mass balance of the terminal-lateral fluctuations of San Rafael Glacier, the Northern Patagonia Icefield, Bulletin of Glacier Research, 6, 55–63, 1988.

Lliboutry, L.: Glaciers of the Wet Andes, in: Satellite Image Atlas of Glaciers of the World, South America, edited by: Williams, R. and Ferringo, J., United States Geological Survey, Professional Papers 1386-I, http://pubs.usgs.gov/prof/p1386i/index.html, 1999.

Maas, H.-G., Schwalbe, E., Dietrich, R., Bässler, M., and Ewert, H.: Determination of spatio-temporal velocity fields on glaciers in West-Greenland by terrestrial image sequence analysis, IAPRS Vol. XXXVII, Part B8, 1419–1424, 2008.

Masiokas, M., Rivera, A., Espizua, L., Villalba, R., Delgada, S., and Aravena, J.: Glacier fluctuations in extratropical South America during the past 1000 years, Palaeogeogr. Palaeocl., 281, 242–268, 2009.

Naruse, R.: Characteristics of Velocity Distribution in Patagonian Glaciers, Geophysical Bulletin of Hokkaido University, Sapporo, No. 49, 211–219, 1987.

Rasmussen, L., Conway, H., and Raymond, F.: Influence of upper air conditions on the Patagonia icefields, Global Planet. Change, 59, 203–216, 2007.

TCD
4, 2415–2432, 2010

Rignot, E., Forster, R., and Isacks, B.: Interferometric radar observations of Glaciar San Rafael, Chile, J. Glaciol., 42(141), 279–291, 1996.
Rignot, E., Rivera, A., and Casassa, G.: Contribution of the Patagonia icefields of South America to global sea level rise, Science, 302, 434–437, 2003.
Rivera, A., Benham, T., Casassa, G., Bamber, J., and Dowdeswell, J.: Ice elevation and areal changes of glaciers from the Northern Patagonia Icefield, Chile, Global Planet. Change, 59(1–4), 126–137, 2007.
Schneider, D. and Maas, H.-G.: Integrated Bundle Adjustment of Terrestrial Laser Scanner Data and Image Data with Variance Component Estimation, The Photogrammetric Journal of Finland, 20, 5–15, 2007.
Thomas, R. Tide-induced perturbations of glacier velocities, Global Planet. Change, 59, 217–224, 2007.
Warren, C.: Rapid recent fluctuations of the calving San Rafael Glacier, Chilean Patagonia: Climatic or non-climatic?, Geografiska Annaler, 75A(3), 111–125, 1993.
Warren, C., Glasser, N., Harrison, S., Winchester, V., Kerr, A., and Rivera, A.: Characteristics of tide-water calving at Glaciar San Rafael, Chile, J. Glaciol., 41(138), 273–289, 1995.

TCD
4, 2415–2432, 2010

Fig. 1. Glaciar San Rafael and Laguna San Rafael.

TCD
4, 2415–2432, 2010

Fig. 2. Glaciar San Rafael front seen from the Laguna San Rafael. The glacier width is 1.8 km.

TCD
4, 2415–2432, 2010

Fig. 3. Example of a glacier surface image section used for feature tracking.

TCD
4, 2415–2432, 2010

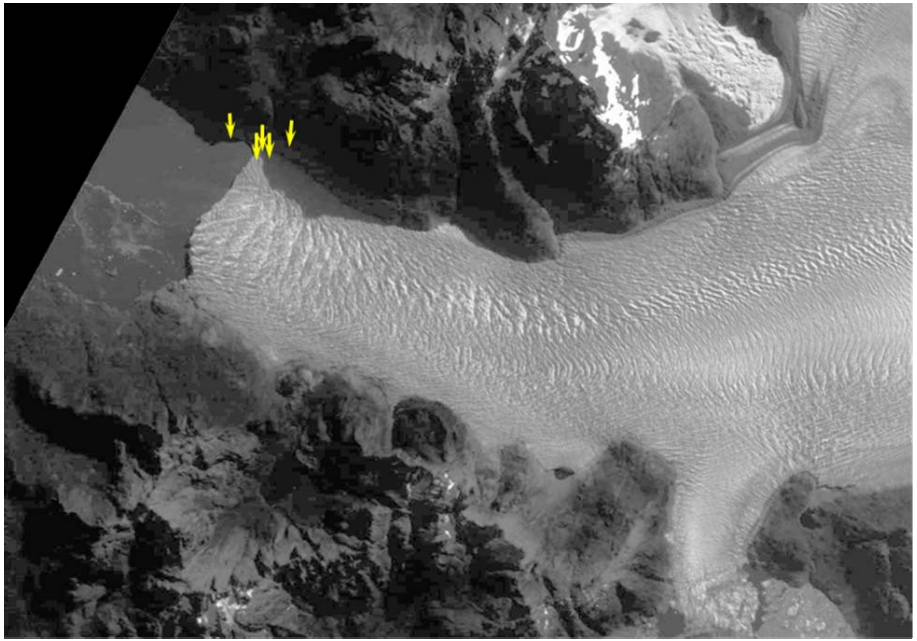

Fig. 4. Multi-station photogrammetric network configuration. Each arrow represents the viewing direction for each of the 5 GPS-supported camera positions.

TCD
4, 2415–2432, 2010

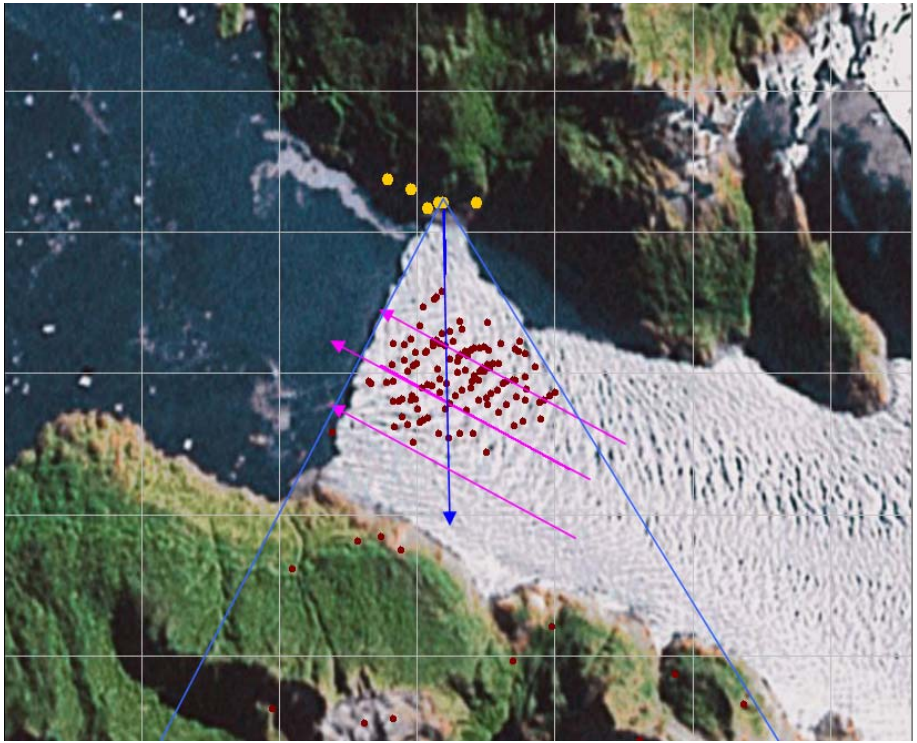

Fig. 5. Intervallometer camera field of view (blue), tracked points (red) and photogrammetric network camera stations (yellow) overlaid on a satellite image with a 1 km grid.

TCD
4, 2415–2432, 2010

Fig. 6. Glacier surface point tracking results.

TCD
4, 2415–2432, 2010